Extended Abstracts of the 2003 International Conference on Solid State Devices and Materials, Tokyo, 2003, pp. 336-337

F-3-2 (Invited)

Type-II InAs-based Quantum Cascade Lasers

K. Ohtani and H. Ohno

Laboratory for Electronic Intelligent Systems, Research Institute of Electrical Communication, Tohoku University
Katahira 2-1-1, Aoba-ku, Sendai, Miyagi 980-8577, Japan
Phone: +81-22-217-5555 E-mail: keita@riec.tohoku.ac.jp

1. Introduction

Type-II InAs/AlGaSb quantum well structures (QWs) have properties advantageous for the operation of intersubband quantum cascade lasers (QCLs) [1]. Its high conduction-band offset energy of 2.1eV offers widely tunable intersubband emission energies [2]. Also large optical gain can be expected due to an increased optical dipole matrix element and a small nonradiative relaxation rate. Although intersubband electroluminescence from InAs/AlGaSb quantum cascade structures was reported earlier [3, 4, 5], there has been no report on InAs/AlGaSb QCLs. Recently, we have successfully observed lasing from an InAs/AlSb QCLs [6, 7]. Here we describe the active region design, molecular beam epitaxy growth, and properties of InAs/AlSb QCLs.

2. Active Region Design

Fig. 1 shows a conduction band-diagram of the injector/active/injector layers in the active region of the device under an electric field of 29 kV/cm. Our previous experimental results indicate that it is necessary to reduce the operating electric fields to avoid band-to-band tunneling in cascade structures containing narrow gap semiconductor such as InAs [8]. In order to reduce the operating electric field, the active region is designed for a longer wavelength emission than the previous attempts, as the electric field at which the injector aligns is inversely proportional to the emission wavelength; here, the designed emission wavelength is 10 μm, which is about two times longer than that of our previous cascade structures (4-6 μm). Since the lifetime of the excited state becomes shorter by approaching the LO phonon energy (30 meV) in the relevant wavelength region, the fast carrier extraction from the ground state is critical in obtaining population inversion between the intersubband states. We have chosen bound-to-continuum transition, where the active optical transition occurs from a bound QW state to a miniband continuum ensuring fast extraction of carriers [9]. In addition, in order to increase the lifetime of the excited state, the active transition is designed to be spatially indirect.

3. Molecular Beam Epitaxy Growth

InAs/AlSb QCLs are grown on n-InAs (100) substrate by a molecular beam epitaxy (MBE) system equipped with an As valved cracker cell and an Sb cracker cell. An InAs double plasmon waveguide structure is used for the optical confinement [10]. After the surface oxide removal, a 1.0 μm bottom high-doped n-InAs cladding region ($3x10^{18}$ cm^{-3}) is grown. The active region is sandwiched between two 3.5 μm low-doped n-InAs core regions ($2x10^{16}$ cm^{-3}). The active region consists of 40-repeated cascade structures shown in Fig. 1 and total thickness of the region is 2.86 μm. After growth of the top low-doped n-InAs core region, a 1.0 μm top high-doped n-InAs cladding region ($3x10^{18}$ cm^{-3}) is grown. During the MBE growth, the substrate temperature is kept at 410 °C. The V/III beam equivalence pressure ratio for the active region is 5 for both InAs growth and AlSb growth. In order to decrease strain associated with lattice mismatch, AlAs interface bonds are adopted at each interface by controlling the shutter sequence.

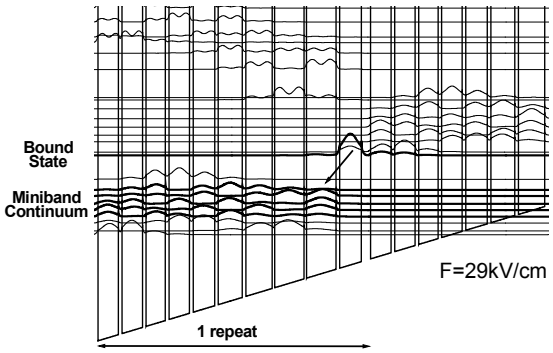

Fig. 1 Schematic band diagram of injector/active/injector under the external field of 29KV/cm.

4. Lasing Properties

Fig. 2 shows the current-light output (*I-L*) characteristics of two devices (device A and B) measured at 4 K. The stripe width of the devices is 30 μm and the stripe length is 0.9 mm. The *I-L* characteristics are measured using voltage pulse at 5 kHz with a duty cycle of 0.05 %. At approximately 5 kA/cm^2, the emission intensity increases abruptly by at least 3 orders of magnitude. The threshold current density is 4.9 kA/cm^2 for device A and 5.2 kA/cm^2 for device B. The inset of Fig. 2 shows the current-voltage characteristic of device A. As expected from the design, current starts to flow at bias of 5 V, at which the injector aligns.

Fig. 3 shows the emission spectra of device A at 4 K. Electroluminescence spectra below threshold are included for comparison, for which a high duty cycle of 5 % is used. By increasing the current density, the emission peak shows a blue shift, which is due to the spatially indirect nature of

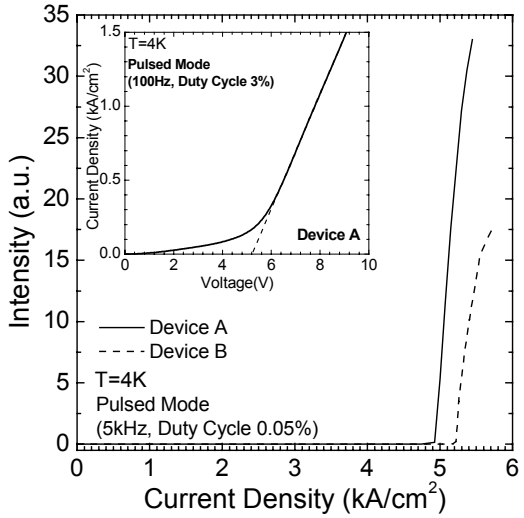

Fig. 2 Current-light output (*I-L*) characteristics of the InAs/AlSb QCLs measured at 4K. Inset shows current-voltage (*I-V*) characteristics of device A at 4K.

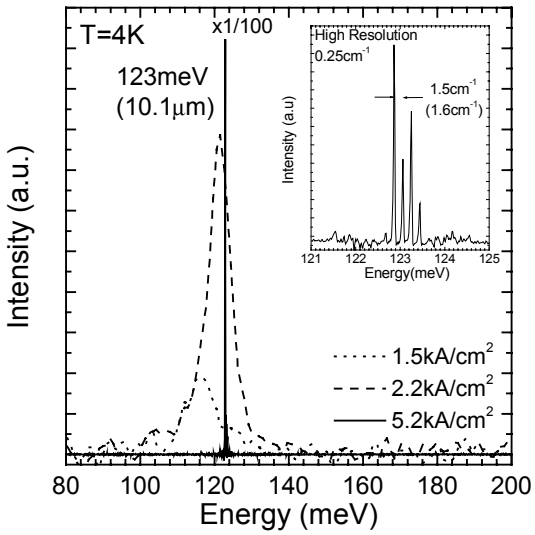

Fig. 3 Emission spectra of device A at 4K measured with a step-scan Fourier transform infrared spectrometer with a lock-in detection technique.

the active transition. Above threshold, the line narrowing of the emission spectra is observed being a direct evidence of the laser action. The observed emission energy is 123 meV corresponding to the wavelength of 10.1 μm, which is in good agreement with the calculated transition energy (115 meV) using a multi-band *k·p* theory. Both electroluminescence and laser emission are polarized normal to the layers, consistent with the intersubband selection rule. The inset of Fig. 3 shows the high-resolution (0.25 cm^{-1}) laser emission spectrum at 5.2 kA/cm^2 taken using a rapid scan mode. Additional higher order transverse modes emerge at the higher injection current density. The observed mode spacing is 1.5 cm^{-1}, in close agreement with the expected value of 1.6 cm^{-1} calculated using the cavity length and the effective refractive index of the waveguide.

5. Conclusions

We have reported design, molecular beam epitaxy growth, and properties of QCLs based on the InAs/AlSb material system. The intersubband transition was chosen to be bound-to-continuum and the InAs double plasmon waveguide was employed for optical confinement. The observed lowest threshold current density is 4.9 kA/cm^2 at 4 K. The laser emission wavelength is 10.1 μm, which is in agreement with the calculated transition energy.

Acknowledgements

The authors thank H. Sakuma for helpful discussion. This work is partly supported by the Telecommunications Advancement Organization (TAO) of Japan and Grant-in-Aids for Scientific Research from the Ministry of Education, Science, Sports, and Culture. Supports at the early stage of the study by the Murata Science Foundation, and the Mazda Foundation are also acknowledged.

References

[1] H. Ohno, L. Esaki, and E. E. Mendez, Appl. Phys. Lett. **60**. 3153 (1992).

[2] K. Ohtani, N. Matsumoto, H. Sakuma, and H. Ohno, Appl. Phys. Lett. **82**, 37 (2003)

[3] K. Ohtani and H. Ohno, Appl. Phys. Lett. **74**, 1409 (1999).

[4] K. Ohtani and H. Ohno, Electron. Lett. **35**, 935 (1999).

[5] K. Ohtani, H. Sakuma, and H. Ohno, Appl. Phys. Lett. **78**, 4148 (2001)

[6] K. Ohtani and H. Ohno, Jpn. J. Appl. Phys. **41**, L1279 (2002)

[7] K. Ohtani and H. Ohno, Appl. Phys. Lett. **82**, 1003 (2003)

[8] K. Ohtani, H. Sakuma, and H. Ohno, J. Crystal. Growth, **251**, 718 (2003)

[9] J. Faist, M. Beck, T. Aellen, and E. Gini, Appl. Phys. Lett. **78**, 147 (2001).

[10] C. Sirtori, P. Kruck, S. Barbieri, H. Page, J. Nagle, M. Beck, J. Faist, U. Oesterle, Appl. Phys. Lett. **75**, 3911 (1999).